Partial Differential Equations in Applied Mathematics 11 (2024) 100783

Contents lists available at ScienceDirect

Partial Differential Equations in Applied Mathematics

journal homepage: www.elsevier.com/locate/padiff

Analytical solutions and soliton behaviors in the space fractional Heisenberg ferromagnetic spin chain equation

Sujoy Devnath [a], Mst. Munny Khatun [b], M. Ali Akbar [c,*]

[a] Department of Electrical and Electronic Engineering, Daffodil International University, Dhaka, Bangladesh
[b] Department of Mathematics, Khulna University of Engineering & Technology, Bangladesh
[c] Department of Applied Mathematics, University of Rajshahi, Bangladesh

ARTICLE INFO

Keywords:
Heisenberg ferromagnetic spin chain model
The extended Kudryashov method
The $(G'/G,\ 1/G)$-expansion method
Beta derivative
Soliton

ABSTRACT

This study investigates soliton solutions to the (2 + 1)-dimensional space fractional Heisenberg ferromagnetic spin chain equation incorporating beta fractional derivatives that explain the nonlinear propagation of spin wave in the ferromagnetic material with magnetic interactions including the both classical and semi-classical frameworks. This model has applications in spintronics, plasma physics, magnet theory, and condensed matter physics. Employing the two-potential extended Kudryashov and $(G'/G,\ 1/G)$-expansion methods, we derive some original and generic solutions composed of trigonometric functions, hyperbolic functions, and their rational forms. For particular values of the parameters, these solutions offer V-shaped, bell-shaped, kink, periodic, flat kink, and singular periodic solitons. The physical behavior of these solitons is demonstrated through three-dimensional, contour, and two-dimensional plots. The results are important in the study of phase transitions in ferromagnetic materials, lattice vibrations in condensed matter, and the propagation of shock waves in plasma. This study also demonstrates the potential and reliability of the employed strategies.

1. Introduction

In recent times, numerous potent and competent studies have surfaced, exploring nonlinear models across various engineering and physical disciplines, such as water waves, signal processing, plasma physics, condensed matter physics, optical fibers, quantum mechanics, and more.[1–8] Understanding the nonlinear phenomena of a system requires the corresponding exact wave solutions. But the study of nonlinear models has been a significant challenge over the years. The resolution to this intriguing problem came with John Scott Russell's discovery of solitary waves, a special type of traveling wave. Solitary waves exhibit notable virtues, including resilience, stability, and the capacity to maintain their shape and velocity even after interacting with others.[9] Scholars have focused a great deal of attention on the unique characteristics of solitons, providing several strategies for generating soliton solutions to nonlinear models.

The nonlinear fractional order evolution equations are the generalization of integer-order equations, offering more realistic and satisfactory outcomes in various nonlinear phenomena. They proved effective in characterizing viscoelastic behavior with fewer parameters,[10] providing insights into the behavior, stability, and unpredictability of chaotic systems,[11] accurate predictions of contaminant transport on anomalous surfaces at large scales,[12] analyzing the variable memory effects in complex physical systems[13] and applications in image processing.[14] Various definitions of fractional order derivatives, such as the Grunwald-Letnikov fractional derivative (FD), Riesz FD, Caputo FD, Yang local fractional derivative, Jumarie's modified Riemann-Liouville FD, conformal FD, beta FD, Riemann-Liouville FD, etc., have been proposed by researchers over the years.[15–19] Some definitions, like the Riemann-Liouville FD, Caputo FD, and conformal FD, have some drawbacks.[17,20] However, the beta FD, introduced by Atangana et al.[19] has not exhibited any deficiencies to date.

Beta derivative: Assuming a function $\mathscr{H}(\xi):[0,\infty)\to\mathbb{R}$, then the beta derivative with respect to ξ of $\mathscr{H}(\xi)$ represented as $D_\xi^\mu\mathscr{H}(\xi)$ and stated as:[19]

$$D_\xi^\mu\mathscr{H}(\xi)=\lim_{\delta\to 0}\frac{\mathscr{H}\left(\xi+\delta\left(\xi+\frac{1}{\Gamma(\mu)}\right)^{1-\mu}\right)-\mathscr{H}(\xi)}{\delta},0<\mu\le 1. \tag{1.1}$$

The definition (1.1) can be also expressed with integer order differential operator as:

* Corresponding author.
E-mail address: ali_math74@yahoo.com (M.A. Akbar).

https://doi.org/10.1016/j.padiff.2024.100783
Received 29 May 2024; Received in revised form 20 June 2024; Accepted 28 June 2024
Available online 29 June 2024

$$D_{\xi}^{\mu}\mathscr{H}(\xi)=\left(\xi+\frac{1}{\Gamma(\mu)}\right)^{1-\mu}\frac{d\mathscr{H}(\xi)}{d\xi}.$$

The following fundamental characteristics of conventional calculus for the beta derivative can be easily proved[21]:

1. Derivative of a constant: $D_{\xi}^{\mu}C=0$, where C is a constant.
2. Linear property: $D_{\xi}^{\mu}[\Phi(\xi)+\Psi(\xi)]=D_{\xi}^{\mu}\Phi(\xi)+D_{\xi}^{\mu}\Psi(\xi)$.
3. Product rule: $D_{\xi}^{\mu}(\Phi(\xi)\Psi(\xi))=\Phi(\xi)D_{\xi}^{\mu}\Psi(\xi)+\Psi(\xi)D_{\xi}^{\mu}\Phi(\xi)$.
4. Quotient rule: $D_{\xi}^{\mu}\frac{\Phi(\xi)}{\Psi(\xi)}=\frac{\Psi(\xi)D_{\xi}^{\mu}\Phi(\xi)-\Phi(\xi)D_{\xi}^{\mu}\Psi(\xi)}{\Psi(\xi)^{2}}$.
5. Chain rule: $D_{\xi}^{\mu}\Phi(\Psi(\xi))=\left(\xi+\frac{1}{\Gamma(\mu)}\right)^{1-\mu}\frac{d\Phi(\Psi(\xi))}{d\Psi(\xi)}.\ \frac{d\Psi(\xi)}{d\xi}$.

The (2 + 1)-dimensional Heisenberg ferromagnetic spin chain (HFSC) equation is a nonlinear Schrödinger type equation that explains the nonlinear spin wave propagation in the ferromagnetic system with magnetic interactions having classical and semi-classical frameworks.[22] This equation has become a fascinating area of research in both mathematics and physics for its practical applications in fields such as spintronics, plasma physics, modern magnet theory, and condensed matter physics. Also, this spin wave has been used to develop reservoir device on a chip.[23] Latha and Vasanthi have derived the (2 + 1)-dimensional HFSC model considering both anisotropic bilinear interactions, which is applicable in the semi-classical framework.[24] The (2 + 1)-dimensional space fractional HFSC equation can be expressed as follows[25]:

$$iV_t+\gamma_1 D_x^{2\mu}V+\gamma_2 D_y^{2\mu}V+\gamma_3 D_{yx}^{2\mu}V-\gamma_4|V|^2V(x,y,t)=0,0<\mu\leq 1, \quad (1.2)$$

where V signifies the coherent amplitudes of spatial coordinate x, y and the temporal coordinate t. γ_1, γ_2, γ_3 and γ_4 are known as the magnetic coupling coefficients and hold the following relations:

$$\gamma_1=\sigma^4(J+J_2),\ \gamma_2=\sigma^4(J_1+J_2),\ \gamma_3=2\sigma^4(J_2)\text{ and }\gamma_4=2\sigma^4(\sim A),$$

where σ denotes the lattice parameter, and the parameters J and J_1 represent bilinear exchange interactions in the xy plane. There is also J_2, which denotes the neighboring interaction throughout the diagonal, and $\sim A$, which indicates the uniaxial crystal field anisotropy coefficient. The model (1.2) incorporates dispersive terms denoted as γ_1, γ_2, and γ_3 along with the Kerr-nonlinearity coefficient γ_4. Previous research has already achieved significant soliton solutions to the (2 + 1)-dimensional HFSC equation for both fractional and integer orders. Bakicierler et al.[22] derived trigonometric, hyperbolic, and rational solutions using the modified extended tanh-function strategy; Uddin et al.[26] derived the soliton solutions using the generalized exponential expansion and the modified Kudryashov methods by varying the beta derivative parameter; the auxiliary equation method along with conformal derivative is employed by Houwe et al.[25], Seadawy et al.[27] constructed dark, bright, and combined bright-dark solitons, solitary waves, periodic waves, and elliptic solutions through improved auxiliary equation and generalized Riccati mapping methods; Hashemi[28] utilized the simplest equation method and Nucci's method with conformal derivative; Hosseini et al.[29] developed 1-soliton solutions with exponential methods and others in.[30–34] Besides the aforementioned applied techniques, there are many other effective and advanced approaches to extract soliton solutions to the nonlinear fractional evolution equations. These techniques include, improved $\exp(-F(\eta))$ -expansion method,[35] the rational (G'/G)-expansion approach,[36] the enhanced modified simple equation scheme,[37] the $(G'/G,1/G)$-expansion method,[38,39] the generalized Kudryashov procedure,[40] the extended Kudryashov technique,[4] the generalized bifurcation method,[41] the Riccati-Bernoulli sub-ODE method,[42] Hirota's methods,[43–45] the improved modified extended Tanh-function method,[46] and so on.

However, to date, no studies have been found that explore soliton solutions for both the integer-order and fractional order HFSC equations through the efficient extended Kudryashov (eK) and $(G'/G,1/G)$-expansion approaches. The aim of the present research is to derive soliton solutions for the fractional HFSC equation using these potential methods along with the beta derivative. We obtain soliton solutions in trigonometric, hyperbolic, and rational forms, some of which align with existing results for specific value of the arbitrary parameters while others are novel and expand the current literature. These novel and generic solutions offer V-shaped solitons, periodic solitons, singular periodic solitons, singular bell-shaped solitons, kink solitons, and flat kink solitons. These derived solutions have potential applications. For example, kink solitons are important in the study of phase transitions in ferromagnetic materials; periodic solitons describe lattice vibrations in condensed matter; and bell-shaped solitons are useful in the study of the propagation of shock waves in plasma.

The article is organized as follows: Section 2 outlines the working procedures of the two methods. In Section 3, the application of these methods is discussed, followed by a comparison with earlier studies in Section 4. Section 5 presents the findings in graphical form, providing physical interpretations. The concluding remarks are presented in the last section.

2. Methodology

In this part, we discuss the key techniques used in the methodologies for the analytical study of fractional order nonlinear evolution (FNLE) equations.

Assume the following FNLE equation:

$$P\left(\chi,\ D_t^{\mu}\chi, D_{x_1}^{\mu}\chi, D_{x_2}^{\mu}\chi,\ldots,D_{tt}^{2\mu}\chi, D_{x_1,\ x_1}^{2\mu}\chi,\ D_{x_1x_2}^{2\mu}\chi\ldots\right)=0,0<\mu<1, \quad (2.1)$$

where P is a polynomial of χ and its fractional or integer-order partial derivatives and χ is the function of spatial variables $x_1,x_2,x_3,\ldots x_n$, and temporal variable t. The parameter μ in $D_{x_1}^{\mu}\chi$ indicates the order of the fractional derivative. The traveling wave transformation converts FNLE (2.1) into a differential equation of a single independent variable. The traveling wave transformation is:

$$\chi(x_1,\ x_2,\ x_3,\ \ldots x_n,\ t)=u(\rho)e^{i\theta(x_1,\ x_2,\ x_3,\ \ldots x_n,\ t)}, \quad (2.2)$$

along with $\rho=\frac{k_1}{\mu}\left(t+\frac{1}{\Gamma\mu}\right)^{\mu}+\frac{k_2}{\mu}\left(x_2+\frac{1}{\Gamma\mu}\right)^{\mu}+\ \ldots+\frac{k_n}{\mu}\left(x_n+\frac{1}{\Gamma\mu}\right)^{\mu}-\frac{\nu}{\mu}\left(t+\frac{1}{\Gamma\mu}\right)^{\mu}$ and

$\theta(x_1,\ x_2,\ x_3,\ \ldots x_n,\ t)=\frac{\sigma_1}{\mu}\left(x_1+\frac{1}{\Gamma\mu}\right)^{\mu}+\frac{\sigma_2}{\mu}\left(x_2+\frac{1}{\Gamma\mu}\right)^{\mu}+\ \ldots+\frac{\sigma_n}{\mu}\left(x_2+\frac{1}{\Gamma\mu}\right)^{\mu}-\frac{\omega}{\mu}\left(t+\frac{1}{\Gamma\mu}\right)^{\mu}$. The amplitude of the new wave function is u(ρ), and its phase is represented by θ($x_1,x_2,x_3,\ldots x_n,t$). Additionally, ν and ω are used to symbolize the wave velocity and wave number, respectively. Using transformation (2.2), Eq. (2.1) results in the following differential equation of u(ρ):

$$Q(u,\ u',\ u'',\ u'''\ldots)=0. \quad (2.3)$$

The key steps of the methodologies for extracting the analytical solutions to Eq. (2.3) are presented below.

2.1. The extended Kudryashov method

Step 1: This strategy provides the following series solution for Eq. (2.3)

$$u(\rho)=C_0+\sum_{l=1}^{N}\sum_{i+k=l}C_{ik}\Phi(\rho)^{i}\ \Psi(\rho)^{k}+\sum_{l=1}^{N}\sum_{i+k=l}D_{ik}\Phi(\rho)^{-i}\ \Psi(\rho)^{-k}, \quad (2.4)$$

where the constants C_0, C_{ik}, D_{ik}, (i, $k=1$, 2, 3…N) are to be calculated. The two functions, Φ(ρ) and Ψ(ρ), that satisfy specific equations of differential calculus. $\Phi(\rho)$ satisfies the Riccati differential equation, while $\Psi(\rho)$ satisfies the Bernoulli differential equation. The Bernoulli differential equation:

$$\Psi'(\rho) = -R_1\Psi(\rho) + R_2\Psi^2(\rho), R_2 \neq 0, \tag{2.5}$$

and the Riccati equation is

$$\Phi'(\rho) = S_0 + S_1\Phi(\rho) + S_2\Phi^2(\rho), S_2 \neq 0, \tag{2.6}$$

where the coefficients S_0,S_1,S_2,R_1,R_2 and β are real constants. The solutions of Bernoulli and Riccati equations are

$$\Psi(\rho) = \begin{cases} \dfrac{-1}{R_2\rho + \beta}, & R_1 = 0, \\ \dfrac{R_1}{R_2 + R_1 exp(R_1\rho + \beta)}, & R_1 \neq 0, \end{cases} \tag{2.7}$$

and

$$\Phi(\rho) = \begin{cases} \dfrac{-S_1}{2S_2} - \dfrac{\sqrt{\alpha}}{2S_2}\tanh\left(\dfrac{\sqrt{\alpha}}{2}\rho + \beta\right), & \alpha > 0, \\ \dfrac{-S_1}{2S_2} - \dfrac{\sqrt{\alpha}}{2S_2}\coth\left(\dfrac{\sqrt{\alpha}}{2}\rho + \beta\right), & \alpha > 0, \\ \dfrac{-S_1}{2S_2} + \dfrac{\sqrt{-\alpha}}{2S_2}\tan\left(\dfrac{\sqrt{-\alpha}}{2}\rho + \beta\right), & \alpha < 0, \\ \dfrac{-S_1}{2S_2} - \dfrac{\sqrt{-\alpha}}{2S_2}\cot\left(\dfrac{\sqrt{-\alpha}}{2}\rho + \beta\right), & \alpha < 0, \\ \dfrac{-S_1}{2S_2} + \dfrac{-1}{S_2\rho + \beta}, & \alpha = 0, \end{cases} \tag{2.8}$$

respectively, where $\alpha = S_1^2 - 4S_0S_2$.

Step 2: The goal of this approach is to discover the soliton solution, which arises when the greatest-order derivative in Eq. (2.3) balances with the nonlinear part. N, which is a positive integer, is obtained from this homogeneous balance in Eq. (2.3).

Step 3: After inserting (2.4) into (2.3) along with (2.5) and (2.6), we obtain a polynomial of $\Phi^\lambda(\rho)\Psi^\varepsilon(\rho)$, ($\lambda$, ε = 1, 2, 3, …). Then, we formulate an algebraic system of equations by setting each coefficient of $\Phi^\lambda(\rho)\Psi^\varepsilon(\rho)$, ($\lambda$, ε = 1, 2, 3, …) in the polynomial to zero. Calculate the values of the coefficients C_0, C_{ik} andD_{ik}, (i, k = 1, 2, 3…N) of the solution (2.4) by solving the algebraic system of equations. Consequently, soliton solution to the FNLE Eq. (2.1) is attained after substituting the transformation (2.2) to the solution (2.4).

2.2. The $(G'/G,1/G)$-expansion method

Step 1: According to this method, the trial solution of the derived Eq. (2.3) is formulated as follows:

$$V(\rho) = \sum_{j=0}^{N} a_j(G'/G)^j + \sum_{j=1}^{N} b_j(G'/G)^{j-1}(1/G), \tag{2.9}$$

where j is a positive integer found using the balance principle along with constants a_j and b_j. $G = G(\rho)$ in Eq. (2.9) will satisfy the subsequent equation of second-order:

$$G''(\rho) + \varepsilon G(\rho) = \delta, \tag{2.10}$$

where λ and δ signify arbitrary parameters. The following relationships can be evaluated

$$\Upsilon' = -\Upsilon^2 + \delta\Theta - \varepsilon, \Theta' = -\Upsilon\Theta, \tag{2.11}$$

with $\Upsilon(\rho) = G'/G$, $\Theta(\rho) = 1/G$.

Three cases arise from the general solution of Eq. (2.10), and they are:

Case 1: The general solution of Eq. (2.10) consists of the following combination of the following trigonometric functions, for $\varepsilon > 0$:

$$G(\rho) = g_1\sin\left(\sqrt{\varepsilon}\ \rho\right) + g_2\cos\left(\sqrt{\varepsilon}\ \rho\right) + \frac{\delta}{\varepsilon}, \tag{2.12}$$

along with $\Theta^2 = \frac{\varepsilon\left(\Upsilon^2 - 2\delta\Theta + \varepsilon\right)}{\varepsilon^2\sigma - \delta^2}$, $\sigma = g_1^2 + g_2^2$, and the arbitrary constants g_1, g_2.

Case 2: When $\varepsilon < 0$, the hyperbolic functions constructed the general solution of Eq. (2.10) as follows:

$$G(\rho) = g_1\sinh\left(\sqrt{-\varepsilon}\ \rho\right) + g_2\cosh\left(\sqrt{-\varepsilon}\ \rho\right) + \frac{\delta}{\varepsilon}, \tag{2.13}$$

together with $\Theta^2 = -\frac{\varepsilon\left(\Upsilon^2 - 2\delta\Theta + \varepsilon\right)}{\varepsilon^2\sigma + \delta^2}$, where $\sigma = g_1^2 - g_2^2$, and the arbitrary constants g_1, g_2.

Case 3: When $\varepsilon = 0$, the rational algebraic functions constructed the general solution of Eq. (2.10) as follows:

$$G(\rho) = \frac{\delta}{2}\rho^2 + g_1\rho + g_2, \tag{2.14}$$

along with $\Theta^2 = \frac{1}{g_1^2 - 2\delta g_2}\left(\Upsilon^2 - 2\delta\Theta\right)$ and the arbitrary constants g_1, g_2.

Step 2: Substituting the values of $V(\rho)$ and its essential derivatives into (2.3), yield an equation containing $\Upsilon^j(\rho)$, $\Theta^j(\rho)$ as well as their derivatives. By replacing the value of $\Theta^2(\zeta)$ and their derivatives, the higher-order terms of $\Theta(\rho)$ and the derivatives are vanished from the attained equation from the attained equation.

Step 3: By comparing the coefficients of $\Upsilon^j\Theta^i$ ($j = 0, 1, \dots N; i = 0, 1$) on both sides of the attained equation, an algebraic system of equations is obtained. Numerous solutions to the Eq. (2.3) are obtained by solving this system of equations for the coefficients of the solution (2.9). Inserting the wave transformation Eq. (2.2) to these extracted solutions, we obtain our desired solitary wave solutions to FNLE Eq. (2.1).

3. Solutions of the space fractional Heisenberg ferromagnetic spin chain equation

The two approaches described earlier are applied in this section to establish solitary wave solutions to the fractional HFSC equation. Consider the beta traveling wave transformation as follows:

$$V = u(\rho)\ e^{i\theta}, \tag{3.1}$$

where $\rho = \frac{\eta_1}{\mu}\left(x + \frac{1}{\Gamma\mu}\right)^\mu + \frac{\eta_2}{\mu}\left(y + \frac{1}{\Gamma\mu}\right)^\mu - \nu t$, $\theta = \frac{k_1}{\mu}\left(x + \frac{1}{\Gamma\mu}\right)^\mu + \frac{k_2}{\mu}\left(y + \frac{1}{\Gamma\mu}\right)^\mu - \omega t$.

Eq. (3.1) reduces Eq. (1.2) into

$$\left(\omega - k_1^2\gamma_1 - k_2^2\gamma_2 - k_1k_2\gamma_3\right)u(\rho) - \gamma_4 u(\rho)^3 + \left(\gamma_1\eta_1^2 + \eta_2(\gamma_3\eta_1 + \gamma_2\eta_2)\right)u''(\rho)$$

$$-i(\nu - k_2(\gamma_3\eta_1 + 2\gamma_2\eta_2) - k_1(2\gamma_1\eta_1 + \gamma_3\eta_2))u'(\rho) = 0. \tag{3.2}$$

The real and imaginary components of (3.2) yield

$$\left(\omega - k_1^2\gamma_1 - k_2^2\gamma_2 - k_1k_2\gamma_3\right)u(\rho) - \gamma_4 u(\rho)^3 + \left(\gamma_1\eta_1^2 + \eta_2(\gamma_3\eta_1 + \gamma_2\eta_2)\right)u''(\rho) = 0, \tag{3.3}$$

and

$$\nu = k_2(\gamma_3\eta_1 + 2\gamma_2\eta_2) + k_1(2\gamma_1\eta_1 + \gamma_3\eta_2). \tag{3.4}$$

3.1. The eK method

Balancing $u''(\rho)$ with $u(\rho)^3$ in Eq. (3.3), we attain $N = 1$. Consequently, the solution of (3.3) according to (3.4) will be in the following form:

$$u(\rho) = C_0 + C_{1,0}\phi(\rho) + C_{0,1}\psi(\rho) + \frac{D_{1,0}}{\phi(\rho)} + \frac{D_{0,1}}{\psi(\rho)}. \tag{3.5}$$

Inserting (3.5) together with (2.5) and (2.6) into (3.3), we obtain a polynomial of $\Phi^{\lambda}(\rho)\Psi^{\varepsilon}(\rho)$, $(\lambda, \varepsilon = 1, 2, 3, \ldots)$ after multiplying both sides by $\phi(\rho)^3\psi(\rho)^3$. Equating the coefficients of $\Phi^{\lambda}(\rho)\Psi^{\varepsilon}(\rho)$, $(\lambda, \varepsilon = 1, 2, 3, \ldots)$ to zero forms a system of equations. By solving this system for C_0, $C_{1,0}$, $C_{0,1}$, $D_{1,0}$, $D_{0,1}$, ω, yields three sets of coefficients corresponding to various soliton solutions of Eq. (1.2).

Set 1: $C_0 = \frac{\pm S_1\sqrt{\gamma_1\eta_1^2+\eta_2(\gamma_3\eta_1+\gamma_2\eta_2)}}{\sqrt{2}\sqrt{\gamma_4}}$, $C_{0,1} = \frac{\pm\sqrt{2}S_2\sqrt{\gamma_1\eta_1^2+\eta_2(\gamma_3\eta_1+\gamma_2\eta_2)}}{\sqrt{\gamma_4}}$, $D_{1,0} = D_{0,1} = C_{1,0} = 0$,

$\omega = k_1^2\gamma_1 + k_2^2\gamma_2 + k_1k_2\gamma_3 + \frac{1}{2}\alpha\left(\gamma_1\eta_1^2 + \gamma_3\eta_1\eta_2 + \gamma_2\eta_2^2\right)$.

Substituting the coefficient values into solution (3.5) and after some simplification, we obtain:

$$V(x,y,t) = \pm\frac{\sqrt{\alpha}\sqrt{\gamma_1\eta_1^2 + \eta_2(\gamma_3\eta_1 + \gamma_2\eta_2)}\ \tanh\left(\beta + \frac{1}{2}\rho\sqrt{\alpha}\right)}{\sqrt{2}\sqrt{\gamma_4}}\ e^{i\theta}, \alpha > 0. \tag{3.6}$$

$$V(x,y,t) = \pm\frac{\sqrt{\alpha}\sqrt{\gamma_1\eta_1^2 + \eta_2(\gamma_3\eta_1 + \gamma_2\eta_2)}\ \coth\left(\beta + \frac{1}{2}\rho\sqrt{\alpha}\right)}{\sqrt{2}\sqrt{\gamma_4}}\ e^{i\theta}, \alpha > 0. \tag{3.7}$$

$$V\ (x,y,t) = \pm\frac{\sqrt{-\alpha}\sqrt{\gamma_1\eta_1^2 + \eta_2(\gamma_3\eta_1 + \gamma_2\eta_2)}\ \tan\left(\beta + \frac{1}{2}\rho\sqrt{\alpha}\right)}{\sqrt{2}\sqrt{\gamma_4}}\ e^{i\theta}, \alpha < 0. \tag{3.8}$$

$$V(x,y,t) = \pm\frac{\sqrt{-\alpha}\sqrt{\gamma_1\eta_1^2 + \eta_2(\gamma_3\eta_1 + \gamma_2\eta_2)}\ \cot\left(\beta + \frac{1}{2}\rho\sqrt{\alpha}\right)}{\sqrt{2}\sqrt{\gamma_4}}\ e^{i\theta}\alpha < 0. \tag{3.9}$$

$$V(x,y,t) = \pm\frac{\sqrt{2}S_2\sqrt{\gamma_1\eta_1^2 + \eta_2(\gamma_3\eta_1 + \gamma_2\eta_2)}}{(\beta + \rho S_2)\sqrt{\gamma_4}}e^{i\theta}, \tag{3.10}$$

where, $\rho = \frac{\eta_1}{\mu}\left(x + \frac{1}{\Gamma\mu}\right)^{\mu} + \frac{\eta_2}{\mu}\left(y + \frac{1}{\Gamma\mu}\right)^{\mu} - t\{k_2(\gamma_3\eta_1 + 2\gamma_2\eta_2) + k_1(2\gamma_1\eta_1 + \gamma_3\eta_2)\}$,

$\theta = \frac{k_1}{\mu}\left(x + \frac{1}{\Gamma\mu}\right)^{\mu} + \frac{k_2}{\mu}\left(y + \frac{1}{\Gamma\mu}\right)^{\mu} - t\left\{k_1^2\gamma_1 + k_2^2\gamma_2 + k_1k_2\gamma_3 + \frac{1}{2}\alpha\left(\gamma_1\eta_1^2 + \gamma_3\eta_1\eta_2 + \gamma_2\eta_2^2\right)\right\}$, $\alpha = S_1^2 - 4S_0S_2$.

Set 2: $C_0 = \pm\frac{S_1\sqrt{\gamma_1\eta_1^2+\eta_2(\gamma_3\eta_1+\gamma_2\eta_2)}}{\sqrt{2}\sqrt{\gamma_4}}$, $C_{0,1} = C_{1,0} = D_{1,0} = 0$, $D_{0,1} = \pm\frac{\sqrt{2}S_0\sqrt{\gamma_1\eta_1^2+\gamma_3\eta_1\eta_2+\gamma_2\eta_2^2}}{\sqrt{\gamma_4}}$,

$\omega = k_1^2\gamma_1 + k_2^2\gamma_2 + k_1k_2\gamma_3 + \frac{1}{2}\alpha\left(\gamma_1\eta_1^2 + \gamma_3\eta_1\eta_2 + \gamma_2\eta_2^2\right)$.

Upon plugging these values into solution (3.5) and abridging the expression, we derive the subsequent outcomes:

$$V(x,y,t) = \pm\frac{\sqrt{\gamma_1\eta_1^2 + \eta_2(\gamma_3\eta_1 + \gamma_2\eta_2)}\left\{\alpha + S_1\sqrt{\alpha}\tanh\left(\beta + \frac{1}{2}\rho\sqrt{\alpha}\right)\right\}}{\sqrt{2}\sqrt{\gamma_4}\left\{S_1 + \sqrt{\alpha}\ \tanh\left(\beta + \frac{1}{2}\rho\sqrt{\alpha}\right)\right\}}e^{i\theta}, \alpha > 0, \tag{3.11}$$

$$V(x,y,t) = \pm\frac{\sqrt{\gamma_1\eta_1^2 + \eta_2(\gamma_3\eta_1 + \gamma_2\eta_2)}\left\{\alpha + S_1\sqrt{\alpha}\ \coth\left(\beta + \frac{1}{2}\rho\sqrt{\alpha}\right)\right\}}{\sqrt{2}\sqrt{\gamma_4}\left\{S_1 + \sqrt{\alpha}\ \coth\left(\beta + \frac{1}{2}\rho\sqrt{\alpha}\right)\right\}}e^{i\theta}, \alpha > 0, \tag{3.12}$$

$$V(x,y,t) = \pm\frac{\sqrt{\gamma_1\eta_1^2 + \eta_2(\gamma_3\eta_1 + \gamma_2\eta_2)}\left\{\alpha - S_1\sqrt{-\alpha}\tan\left(\beta + \frac{1}{2}\rho\sqrt{-\alpha}\right)\right\}}{\sqrt{2}\sqrt{\gamma_4}\left\{S_1 - \sqrt{-\alpha}\tan\left(\beta + \frac{1}{2}\rho\sqrt{-\alpha}\right)\right\}}e^{i\theta}, \alpha < 0, \tag{3.13}$$

$$V(x,y,t) = \pm\frac{\sqrt{\gamma_1\eta_1^2 + \eta_2(\gamma_3\eta_1 + \gamma_2\eta_2)}\left\{\alpha + S_1\sqrt{-\alpha}\cot\left(\beta + \frac{1}{2}\rho\sqrt{-\alpha}\right)\right\}}{\sqrt{2}\sqrt{\gamma_4}\left\{S_1 + \cot\left(\beta + \frac{1}{2}\rho\sqrt{-\alpha}\right)\sqrt{-\alpha}\right\}}\ e^{i\theta}, \alpha < 0, \tag{3.14}$$

$$V(x,y,t) = \pm\frac{2S_1S_2\sqrt{\gamma_1\eta_1^2 + \eta_2(\gamma_3\eta_1 + \gamma_2\eta_2)}}{\sqrt{2}(2S_2 + S_1(\beta + wS_2))\ \sqrt{\gamma_4}}, e^{i\theta}, \alpha < 0, \tag{3.15}$$

where $\rho = \frac{\eta_1}{\mu}\left(x + \frac{1}{\Gamma\mu}\right)^{\mu} + \frac{\eta_2}{\mu}\left(y + \frac{1}{\Gamma\mu}\right)^{\mu} - t\{k_2(\gamma_3\eta_1 + 2\gamma_2\eta_2) + k_1(2\gamma_1\eta_1 + \gamma_3\eta_2)\}$,

$$\theta = \frac{k_1}{\mu}\left(x + \frac{1}{\Gamma\mu}\right)^{\mu} + \frac{k_2}{\mu}\left(y + \frac{1}{\Gamma\mu}\right)^{\mu} - t\left\{k_1^2\gamma_1 + k_2^2\gamma_2 + k_1k_2\gamma_3 + \frac{1}{2}\alpha\left(\gamma_1\eta_1^2 + \gamma_3\eta_1\eta_2 + \gamma_2\eta_2^2\right)\right\},\ \alpha = S_1^2 - 4S_0S_2.$$

Set 3: $C_0 = \frac{\pm R_1\sqrt{\gamma_1\eta_1^2+\eta_2(\gamma_3\eta_1+\gamma_2\eta_2)}}{\sqrt{2}\sqrt{\gamma_4}}$, $C_{0,1} = D_{1,0} = D_{0,1} = 0$, $C_{1,0} = \frac{\pm\sqrt{2}R_2\sqrt{\gamma_1\eta_1^2+\eta_2(\gamma_3\eta_1+\gamma_2\eta_2)}}{\sqrt{\gamma_4}}$,

$$\omega = k_1^2\gamma_1 + k_2^2\gamma_2 + k_1k_2\gamma_3 + \frac{1}{2}R_1^2\left(\gamma_1\eta_1^2 + \gamma_3\eta_1\eta_2 + \gamma_2\eta_2^2\right).$$

By inserting the values of set 3 into Eq. (3.5) and refining the expression, the resulting solutions are obtained as follows:

$$V(x,y,t) = \pm e^{i\theta}\frac{R_1(e^{\beta+\rho R_1}R_1 - R_2)\sqrt{\gamma_1\eta_1^2 + \eta_2(\gamma_3\eta_1 + \gamma_2\eta_2)}}{\sqrt{2}(e^{\beta+\rho R_1}R_1 + R_2)\sqrt{\gamma_4}}, R_1 \neq 0, \tag{3.16}$$

$$V(x,y,t) = \pm e^{i\theta}\frac{(2R_2 + R_1(\beta + \rho R_2))\sqrt{\gamma_1\eta_1^2 + \eta_2(\gamma_3\eta_1 + \gamma_2\eta_2)}}{\sqrt{2}(\beta + \rho R_2)\sqrt{\gamma_4}}, R_1 = 0, \tag{3.17}$$

where $\rho = \frac{\eta_1}{\mu}\left(x + \frac{1}{\Gamma\mu}\right)^{\mu} + \frac{\eta_2}{\mu}\left(y + \frac{1}{\Gamma\mu}\right)^{\mu} - t\{k_2(\gamma_3\eta_1 + 2\gamma_2\eta_2) + k_1(2\gamma_1\eta_1 + \gamma_3\eta_2)\}$,

$$\theta = \frac{k_1}{\mu}\left(x + \frac{1}{\Gamma\mu}\right)^{\mu} + \frac{k_2}{\mu}\left(y + \frac{1}{\Gamma\mu}\right)^{\mu} - t\left[k_1^2\gamma_1 + k_2^2\gamma_2 + k_1k_2\gamma_3 + \frac{1}{2}R_1^2\left\{\gamma_1\eta_1^2 + \eta_2(\gamma_3\eta_1 + \gamma_2\eta_2)\right\}\right].$$

3.2. The (G′/G, 1/G)-expansion method

Through the application of the homogeneous principle of balance to Eq. (3.3), it can be derived that $N = 1$. Therefore, the solitary wave solution of Eq. (3.3) holds the form:

$$u(\rho) = a_0 + a_1\phi(\rho) + b_1\psi(\rho). \tag{3.18}$$

Employing the major steps asserted in the section of methodology, the following set of solutions have been supplied for Eq. (3.3).

Group 1 ($\lambda < 0$): The obtained solutions for this condition affiliated with the parameter λ are as follows:

Family 1: $a_0 = 0$, $a_1 = \pm\frac{\sqrt{\omega - k_1^2\gamma_1 - k_2^2\gamma_2 - k_1k_2\gamma_3}}{\sqrt{-\lambda}\sqrt{\gamma_4}}$, $b_1 = \pm\frac{\sqrt{\delta^2+\lambda^2\sigma}\left(\sqrt{\omega - k_1^2\gamma_1 - k_2^2\gamma_2 - k_1k_2\gamma_3}\right)}{\lambda\sqrt{\gamma_4}}$,

$k_1 = k_1$, $k_2 = k_2$, $\omega = \omega$, $\nu = k_2(\gamma_3\eta_1 + 2\gamma_2\eta_2) + k_1(2\gamma_1\eta_1 + \gamma_3\eta_2)$, $\eta_2 = -\frac{\lambda\gamma_3\eta_1 + \sqrt{\lambda\left(8k_2^2\gamma_2^2 + \lambda\gamma_3^2\eta_1^2 + \gamma_2\left(-8\omega + 8k_1^2\gamma_1 + 8k_1k_2\gamma_3 - 4\lambda\gamma_1\eta_1^2\right)\right)}}{2\lambda\gamma_2}$.

Family 2: $a_0 = 0$, $a_1 = \pm\frac{\sqrt{\omega - k_1^2\gamma_1 - k_2^2\gamma_2 - k_1k_2\gamma_3}}{\sqrt{-\lambda}\sqrt{\gamma_4}}$, $b_1 = 0$, $\delta = 0$, $\omega = \omega$, $\nu = k_2(\gamma_3\eta_1 + 2\gamma_2\eta_2) + k_1(2\gamma_1\eta_1 + \gamma_3\eta_2)$, $\eta_2 = -\frac{\sqrt{4\lambda^2\gamma_3^2\eta_1^2 - 8\lambda\gamma_2\left(\omega - k_1^2\gamma_1 - k_2^2\gamma_2 - k_1k_2\gamma_3 + 2\lambda\gamma_1\eta_1^2\right)} + 2\lambda\gamma_3\eta_1}{4\lambda\gamma_2}$.

Family 3: $a_0 = 0$, $a_1 = 0$, $b_1 = \pm\frac{\sqrt{-2\sigma\left(\omega - k_1^2\gamma_1 - k_2^2\gamma_2 - k_1k_2\gamma_3\right)}}{\sqrt{\gamma_4}}$, $\delta = 0$, $\nu = k_2(\gamma_3\eta_1 + 2\gamma_2\eta_2) + k_1(2\gamma_1\eta_1 + \gamma_3\eta_2)$, $\eta_2 = \frac{\sqrt{\lambda^2\gamma_3^2\eta_1^2 + 4\lambda\gamma_2\left(\omega - k_1^2\gamma_1 - k_2^2\gamma_2 - k_1k_2\gamma_3 - \lambda\gamma_1\eta_1^2\right)} - \lambda\gamma_3\eta_1}{2\lambda\gamma_2}$.

Utilizing the values of parameters assessed in family 1 to solution (3.18), the originated solution of Eq. (3.3) is

$$u(\rho) = \pm\frac{\sqrt{\omega - k_1^2\gamma_1 - k_2^2\gamma_2 - k_1k_2\gamma_3}}{\lambda\left(\frac{\delta}{\lambda} + \sinh\left(\sqrt{-\lambda}\rho\right)g_1 + \cosh\left(\sqrt{-\lambda}\rho\right)g_2\right)\sqrt{\gamma_4}}\left\{\sqrt{\delta^2+\lambda^2\sigma} - \lambda\left(\cosh\left(\sqrt{-\lambda}\rho\right)g_1 + \sinh\left(\sqrt{-\lambda}\rho\right)g_2\right)\right\}.$$

Therefore, solution of the Eq. (1.2), obtained from the transformation (3.1), has the form:

$$V(x,y,t) = \pm\frac{e^{i\theta}\sqrt{\omega - k_1^2\gamma_1 - k_2^2\gamma_2 - k_1k_2\gamma_3}}{\lambda\left(\frac{\delta}{\lambda} + \sinh\left(\sqrt{-\lambda}\rho\right)g_1 + \cosh\left(\sqrt{-\lambda}\rho\right)g_2\right)\sqrt{\gamma_4}}\{\sqrt{\delta^2+\lambda^2\sigma} - \lambda\left(\cosh\left(\sqrt{-\lambda}\rho\right)g_1 + \sinh\left(\sqrt{-\lambda}\rho\right)g_2\right)\}, \tag{3.19}$$

along with $\rho = \frac{\eta_1}{\mu}\left(x + \frac{1}{\Gamma\mu}\right)^{\mu} + \frac{\eta_2}{\mu}\left(y + \frac{1}{\Gamma\mu}\right)^{\mu} - \nu t$, and $\theta = \frac{k_1}{\mu}\left(x + \frac{1}{\Gamma\mu}\right)^{\mu} + \frac{k_2}{\mu}\left(y + \frac{1}{\Gamma\mu}\right)^{\mu} - \omega t$.

In a similar manner, the remaining solution sets were utilized to produce the subsequent solutions for Eq. (1.2):

$$V(x,y,t) = \pm\frac{e^{i\theta}\left(\cosh\left(\sqrt{-\lambda}\rho\right)g_1 + \sinh\left(\sqrt{-\lambda}\rho\right)g_2\right)\sqrt{\omega - k_1^2\gamma_1 - k_2^2\gamma_2 - k_1k_2\gamma_3}}{\left(\sinh\left(\sqrt{-\lambda}\rho\right)g_1 + \cosh\left(\sqrt{-\lambda}\rho\right)g_2\right)\sqrt{\gamma_4}}, \tag{3.20}$$

and

$$V(x,y,t) = \pm\frac{e^{i\theta}\sqrt{-2\sigma\left(\omega - \sigma k_1^2\gamma_1 - \sigma k_2^2\gamma_2 - \sigma k_1k_2\gamma_3\right)}}{\left(\sinh\left(\sqrt{-\lambda}\rho\right)g_1 + \cosh\left(\sqrt{-\lambda}\rho\right)g_2\right)\sqrt{\gamma_4}}. \tag{3.21}$$

In solutions (3.20) and (3.21), $\rho = \frac{\eta_1}{\mu}\left(x + \frac{1}{\Gamma\mu}\right)^{\mu} + \frac{\eta_2}{\mu}\left(y + \frac{1}{\Gamma\mu}\right)^{\mu} - \nu t$, and $\theta = \frac{k_1}{\mu}\left(x + \frac{1}{\Gamma\mu}\right)^{\mu} + \frac{k_2}{\mu}\left(y + \frac{1}{\Gamma\mu}\right)^{\mu} - \omega t$. Now, if we make the estimation that $\delta = 0$ and $g_2 = 0$, the solution (3.19) takes the form:

$$V(x,y,t) = \pm\frac{e^{i\theta}\sqrt{\omega - k_1^2\gamma_1 - k_2^2\gamma_2 - k_1k_2\gamma_3}}{\sqrt{\gamma_4}}\left\{\operatorname{csch}\left(\sqrt{-\lambda}\rho\right) - \coth\left(\sqrt{-\lambda}\rho\right)\right\}. \tag{3.22}$$

Analogously, the rest of the solution may be altered to another form of solutions.

Group 2 ($\lambda > 0$): The solutions, we have obtained for Eq. (3.3) through the aforementioned method, are as follows:

Family 1: $a_0 = 0$, $a_1 = \pm\frac{\sqrt{-\omega + k_1^2\gamma_1 + k_2^2\gamma_2 + k_1k_2\gamma_3}}{\sqrt{\lambda}\sqrt{\gamma_4}}$, $b_1 = \pm\frac{\sqrt{-\delta^2+\lambda^2\sigma}\left(\sqrt{-\omega + k_1^2\gamma_1 + k_2^2\gamma_2 + k_1k_2\gamma_3}\right)}{\lambda\sqrt{\gamma_4}}$,

$\nu = k_2(\gamma_3\eta_1 + 2\gamma_2\eta_2) + k_1(2\gamma_1\eta_1\gamma_3\eta_2)$, $\eta_2 = -\frac{\sqrt{\lambda^2\gamma_3^2\eta_1^2 - 4\lambda\gamma_2\left(2\omega - 2k_1^2\gamma_1 - 2k_2^2\gamma_2 - 2k_1k_2\gamma_3 + \lambda\gamma_1\eta_1^2\right)} + \lambda\gamma_3\eta_1}{2\lambda\gamma_2}$.

Family 2: $a_0 = 0$, $a_1 = \pm\frac{\sqrt{-\omega + k_1^2\gamma_1 + k_2^2\gamma_2 + k_1k_2\gamma_3}}{\sqrt{\lambda}\sqrt{\gamma_4}}$, $b_1 = 0$, $\delta = 0$, $\nu = k_2(\gamma_3\eta_1 + 2\gamma_2\eta_2) + k_1(2\gamma_1\eta_1 + \gamma_3\eta_2)$, $\eta_2 = -\frac{\sqrt{4\lambda^2\gamma_3^2\eta_1^2 - 8\lambda\gamma_2\left(\omega - k_1^2\gamma_1 - k_2^2\gamma_2 - k_1k_2\gamma_3 + 2\lambda\gamma_1\eta_1^2\right)} + 2\lambda\gamma_3\eta_1}{4\lambda\gamma_2}$.

Family 3: $a_0 = 0$, $a_1 = 0$, $b_1 = \pm\frac{\sqrt{2}\sqrt{\sigma\left(\omega - k_1^2\gamma_1 - k_2^2\gamma_2 - k_1k_2\gamma_3\right)}}{\sqrt{\gamma_4}}$, $\delta = 0$, $\nu = k_2(\gamma_3\eta_1 + 2\gamma_2\eta_2) + k_1(2\gamma_1\eta_1 + \gamma_3\eta_2)$, $\eta_2 = \frac{-\lambda\gamma_3\eta_1 + \sqrt{\lambda^2\gamma_3^2\eta_1^2 + 4\lambda\gamma_2\left(\omega - k_1^2\gamma_1 - k_2^2\gamma_2 - k_1k_2\gamma_3 - \lambda\gamma_1\eta_1^2\right)}}{2\lambda\gamma_2}$.

Applying the values of the parameters stated in family 1 of group 2 to Eq. (3.18) and Eq. (3.1), the obtained solution of Eq. (1.2) is

$$V(x,y,t) = -\frac{e^{i\theta}\sqrt{-\omega + k_1^2\gamma_1 + k_2^2\gamma_2 + k_1k_2\gamma_3}}{\lambda\left(\frac{\delta}{\lambda} + \sin\left(\sqrt{\lambda}\rho\right)g_1 + \cos\left(\sqrt{\lambda}\rho\right)g_2\right)\sqrt{\gamma_4}}\{\sqrt{-\delta^2+\lambda^2\sigma} - \lambda\left(\cos\left(\sqrt{\lambda}\rho\right)g_1 - \sin\left(\sqrt{\lambda}\rho\right)g_2\right)\}. \tag{3.23}$$

Analogously, the other solutions have originated as:

$$V(x,y,t) = -\frac{e^{i\theta}\left(\cos\left(\sqrt{\lambda}\rho\right)g_1 - \sin\left(\sqrt{\lambda}\rho\right)g_2\right)\sqrt{-\omega + k_1^2\gamma_1 + k_2^2\gamma_2 + k_1k_2\gamma_3}}{\left(\sin\left(\sqrt{\lambda}\rho\right)g_1 + \cos\left(\sqrt{\lambda}\rho\right)g_2\right)\sqrt{\gamma_4}}, \tag{3.24}$$

and

$$V(x,y,t) = \frac{e^{i\theta}\sqrt{2}\sqrt{\sigma\left(\omega - k_1^2\gamma_1 - k_2^2\gamma_2 - k_1k_2\gamma_3\right)}}{\left(\sin\left(\sqrt{\lambda}\rho\right)g_1 + \cos\left(\sqrt{\lambda}\rho\right)g_2\right)\sqrt{\gamma_4}}. \tag{3.25}$$

Here $\rho = \frac{\eta_1}{\mu}\left(x + \frac{1}{\Gamma\mu}\right)^{\mu} + \frac{\eta_2}{\mu}\left(y + \frac{1}{\Gamma\mu]}\right)^{\mu} - \nu t$, and $\theta = \frac{k_1}{\mu}\left(x + \frac{1}{\Gamma\mu}\right)^{\mu} + \frac{k_2}{\mu}\left(y + \frac{1}{\Gamma\mu]}\right)^{\mu} - \omega t$.

Group 3 ($\lambda = 0$): The solutions, we have obtained for Eq. (3.3) through the aforementioned method are as follows:

Family 1: $a_0 = 0$, $a_1 = -\frac{\sqrt{\gamma_1\eta_1^2 + \gamma_3\eta_1\eta_2 + \gamma_2\eta_2^2}}{\sqrt{2}\sqrt{\gamma_4}}$, $b_1 = -\frac{\sqrt{g_1^2 - 2\delta g_2}\left(\sqrt{\gamma_1\eta_1^2 + \gamma_3\eta_1\eta_2 + \gamma_2\eta_2^2}\right)}{\sqrt{2}\sqrt{\gamma_4}}$,

$\nu = k_2(\gamma_3\eta_1 + 2\gamma_2\eta_2) + k_1(2\gamma_1\eta_1 + \gamma_3\eta_2)$, $k_1 = \frac{\left(\sqrt{4\omega\gamma_1 - 4k_2^2\gamma_1\gamma_2 + k_2^2\gamma_3^2}\right) - k_2\gamma_3}{2\gamma_1}$.

Table 1
Comparison of the outcomes attained from the eK method to the prior work in.[27]

Results of Seadawy et al.[27]	Results attained in this study
The outcomes in Eq. (37) is: $Q_1(\xi) = -\dfrac{A_0\sqrt{\tau}\tanh\left(\frac{\sqrt{\tau}}{2}\xi\right)}{q}e^{i\phi}$.	When $\beta = 0$, the outcome (3.6) can be represented as: $V(\rho) = \pm\sqrt{\alpha}\,A\tanh\left[\frac{1}{2}\rho\sqrt{\alpha}\right]e^{i\theta}$.
The solution in Eq. (38) is: $Q_2(\xi) = -\dfrac{A_0\sqrt{\tau}\coth\left(\frac{\sqrt{\tau}}{2}\xi\right)}{q}e^{i\phi}$.	When $\beta = 0$, the outcome (3.7) can be represented as: $V(\rho) = \pm\sqrt{\alpha}\,A\coth\left(\frac{1}{2}\rho\sqrt{-\alpha}\right)e^{i\theta}$.
The solution in Eq. (49) is: $Q_{13}(\xi) = -\dfrac{A_0\sqrt{-\tau}\tan\left(\frac{\sqrt{-\tau}}{2}\xi\right)}{q}e^{i\phi}$.	When $\beta = 0$, the outcome (3.8) can be represented as: $V(\rho) = \pm\sqrt{-\alpha}A\tan\left(\frac{1}{2}\rho\sqrt{-\alpha}\right)e^{i\theta}$.
The solution of (50) is: $Q_{14}(\xi) = -\dfrac{A_0\sqrt{-\tau}\cot\left(\frac{\sqrt{-\tau}}{2}\xi\right)}{q}e^{i\phi}$.	When $\beta = 0$, $S_1 = S_2 \neq 0$ the outcome (3.9) can be represented as: $V(\rho) = \pm\sqrt{-\alpha}\,A\cot\left(\frac{1}{2}\rho\sqrt{-\alpha}\right)e^{i\theta}$.

Table 2
Comparison of the outcomes attained from $(G'/G, 1/G)$-expansion scheme to the prior work in.[47]

Solutions of[47]	Solutions of this article
Solution (16) and (17) holds the general form as $\upsilon_{11}(\xi) = \pm\kappa_0\tan\left(\sqrt{\eta}\,\xi\right)e^{i\Omega}$, where κ_0, η = free parameters.	Solution (3.24) of the recent paper takes the general form $V(x,y,t) = \pm a_1\tan(\sqrt{\lambda}\rho)e^{i\theta}$, for $g_1 = 0$.
Solutions (26) and (27) hold the general form $\upsilon_{11}(\xi) = \pm\kappa_0\cot\left(\sqrt{\eta}\,\xi\right)e^{i\Omega}$.	The solution (3.24) of the presented paper takes the general form $V(x,y,t) = \pm a_1\cot(\sqrt{\lambda}\rho)e^{i\theta}$, for $g_2 = 0$.
Solutions (36) and (37) hold the general form $\upsilon_{11}(\xi) = \pm\kappa_1\tanh\left(\sqrt{-\eta}\,\xi\right)e^{i\Omega}$, here, $\kappa_1 = i\kappa_0$.	The solution (3.20) of the presented paper takes the general form $V(x,y,t) = \pm A_1\tanh(\sqrt{-\lambda}\rho)e^{i\theta}$, for $g_1 = 0$, and $A_1 = ia_1$.
Solutions (46) and (47) hold the general form $\upsilon_{11}(\xi) = \pm\kappa_1\coth\left(\sqrt{-\eta}\,\xi\right)e^{i\Omega}$, here, $\kappa_1 = i\kappa_0$.	The solution (3.20) of the presented paper takes the general form $V(x,y,t) = \pm A_1\coth(\sqrt{-\lambda}\rho)e^{i\theta}$, for $g_2 = 0$, and $A_1 = ia_1$.

Family 2: $a_0 = 0$, $a_1 = -\frac{\sqrt{2}\sqrt{\gamma_1\eta_1^2+\gamma_3\eta_1\eta_2+\gamma_2\eta_2^2}}{\sqrt{\gamma_4}}$, $b_1 = 0$, $k_1 = \frac{\left(\sqrt{4\omega\gamma_1-4k_2^2\gamma_1\gamma_2+k_2^2\gamma_3^2}\right)-k_2\gamma_3}{2\gamma_1}$, $\delta = 0$, $\nu = k_2(\gamma_3\eta_1 + 2\gamma_2\eta_2) + k_1(2\gamma_1\eta_1 + \gamma_3\eta_2)$.

Family 3: $a_0 = 0$, $a_1 = 0$, $b_1 = -\frac{\sqrt{2g_1^2\left(\gamma_1\eta_1^2+\gamma_3\eta_1\eta_2+\gamma_2\eta_2^2\right)}}{\sqrt{\gamma_4}}$, $k_1 = -\frac{\sqrt{4\omega\gamma_1-4k_2^2\gamma_1\gamma_2+k_2^2\gamma_3^2}+k_2\gamma_3}{2\gamma_1}$,
$\delta = 0$, $\nu = k_2(\gamma_3\eta_1 + 2\gamma_2\eta_2) + k_1(2\gamma_1\eta_1 + \gamma_3\eta_2)$.

The following solutions are found by entering the above-estimated values of the parameters in Eqs. (3.18) and (3.1).

$$V(x,y,t) = -\frac{e^{i\theta}(\delta\rho + g_1)\sqrt{\gamma_1\eta_1^2 + \gamma_3\eta_1\eta_2 + \gamma_2\eta_2^2}}{\sqrt{2}\left(\frac{\delta\rho^2}{2} + \rho g_1 + g_2\right)\sqrt{\gamma_4}}\left\{(\delta\rho + g_1) - \sqrt{g_1^2 - 2\delta g_2}\right\}, \tag{3.26}$$

$$V(x,y,t) = -\frac{e^{i\theta}g_1\sqrt{2(\gamma_1\eta_1^2 + \gamma_3\eta_1\eta_2 + \gamma_2\eta_2^2)}}{\sqrt{\gamma_4}\,(\rho g_1 + g_2)}, \tag{3.27}$$

$$V(x,y,t) = -\frac{e^{i\theta}\sqrt{2}g_1\sqrt{\gamma_1\eta_1^2 + \gamma_3\eta_1\eta_2 + \gamma_2\eta_2^2}}{(\rho g_1 + g_2)\sqrt{\gamma_4}}, \tag{3.28}$$

where $\rho = \frac{\eta_1}{\mu}\left(x + \frac{1}{\Gamma\mu}\right)^{\mu} + \frac{\eta_2}{\mu}\left(y + \frac{1}{\Gamma\mu}\right)^{\mu} - \nu t$, and $\theta = \frac{k_1}{\mu}\left(x + \frac{1}{\Gamma\mu}\right)^{\mu} + \frac{k_2}{\mu}\left(y + \frac{1}{\Gamma\mu}\right)^{\mu} - \omega t$.

4. A comparison of the results

To verify the uniqueness of the solutions offered, we compare our findings with those from prior studies to assess the effectiveness of the approach in providing novel and reliable solutions. The solutions obtained through the eK method have been compared with those reported in the prior article by Seadawy et al.[27]. The following considerations facilitate the comparison:

For this paper: $A = \frac{\sqrt{\gamma_1\eta_1^2+\eta_2(\gamma_3\eta_1+\gamma_2\eta_2)}}{\sqrt{2}\sqrt{\gamma_4}}$, $\alpha = S_1^2 - 4S_0S_2$.

For the earlier research[27]: $\tau = q^2 - 4pr$, $\phi = \beta_1 x + \beta_2 y + \nu t + \theta$.

Analogously, the obtained solutions through the $(G'/G, 1/G)$-expansion method have been compared with the solutions of the prior article reported in.[47] To proceed this task, we choose the successive values for deducing the general form of the solution, which assists to compare the solution easily. The assumptions are as follows:

For the previous article: $\kappa_0 = \frac{\sqrt{\alpha_4(\alpha_1 p^2+pq\alpha_3+q^2\alpha_2-r}}{\alpha_4}$, $\eta = \frac{(\alpha_1 p^2+pq\alpha_3+q^2\alpha_2-r}{2(\alpha_1 a^2+ab\alpha_3+b^2\alpha_2)}$, $\Omega = px + qy - rt$, $\xi = ax + by - \omega t$.

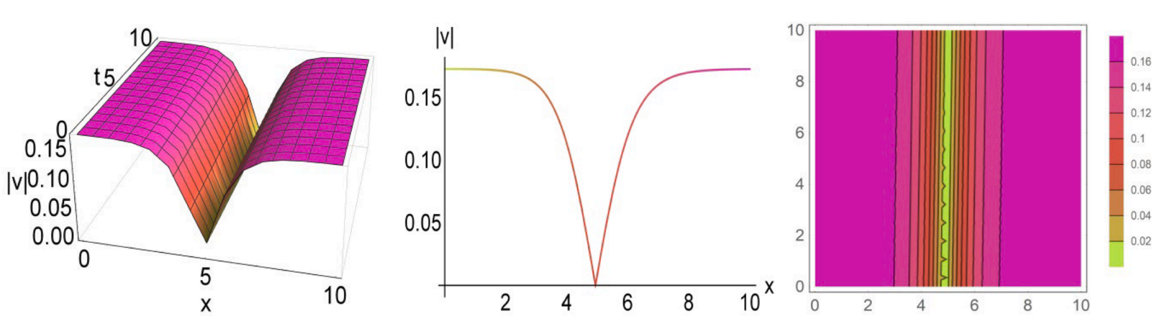

(a) 3D graph. (b) 2D plot for $t = 5$. (c) Contour plot.

Fig. 1. Graphical representation of the absolute component of solution (3.6).

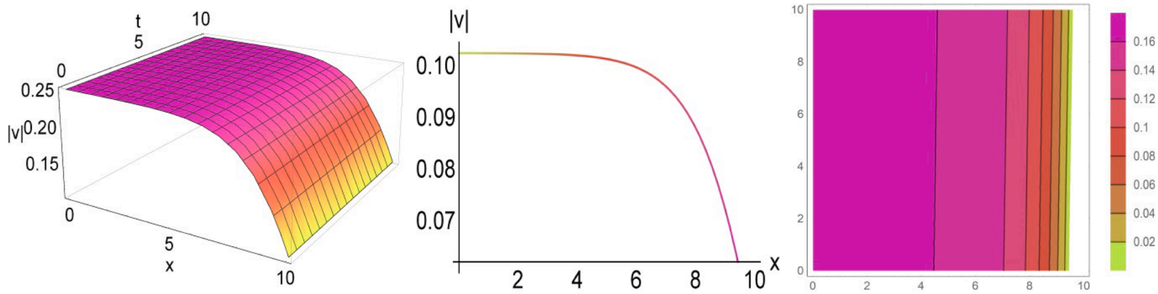

(a) 3D plot. (b) 2D plot for $t = 2$. (c) Contour plot.

Fig. 2. Graphical exhibition of the absolute component of solution (3.6).

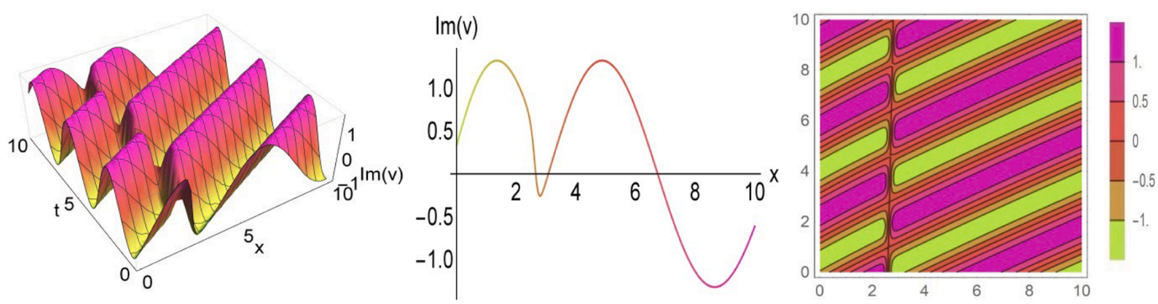

(a) 3D plot. (b) 2D plot for $t = 3$. (c) Contour plot.

Fig. 3. Graphical exhibition of the imaginary component of solution (3.6).

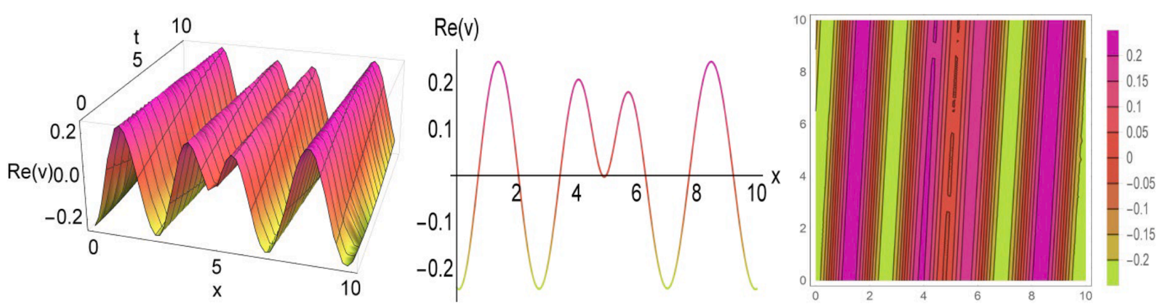

(a) 3D plot. (b) 2D plot for $t = 3$. (c) Contour plot.

Fig. 4. Graphical exhibition of the real component of solution (3.6).

For this article: $a_1 = \pm\frac{\sqrt{-\omega+k_1^2\gamma_1+k_2^2\gamma_2+k_1k_2\gamma_3}}{\sqrt{\gamma_4}}$, $\mu = 1$.

Seadawy et al.[27] employed the Riccati Mapping technique to derive soliton solutions for the HFSC equation. Our comparison with their findings, detailed in Table 1, validates several of their solutions specifically for $\beta = 0$. Additionally, the comparison reveals that the eK approach provides a broader range of rational solutions involving trigonometric and hyperbolic functions, which were not explored in their study. In Table 2, we compare the outcomes from the $(G'/G, 1/G)$-expansion method with the extended rational sine-cosine technique. This comparison highlights that while some of their solutions can

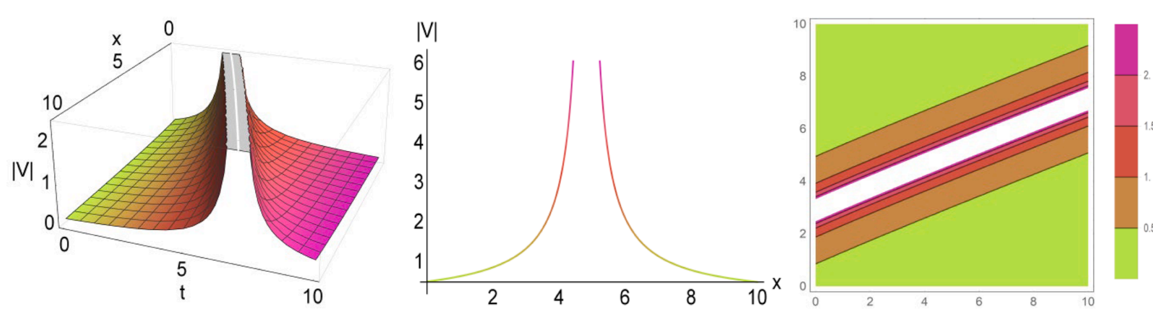

(a) 3D plot. (b) 2D plot for $t = 5$. (c) Contour plot.

Fig. 5. Graphical exhibition of the absolute component of solution (3.17).

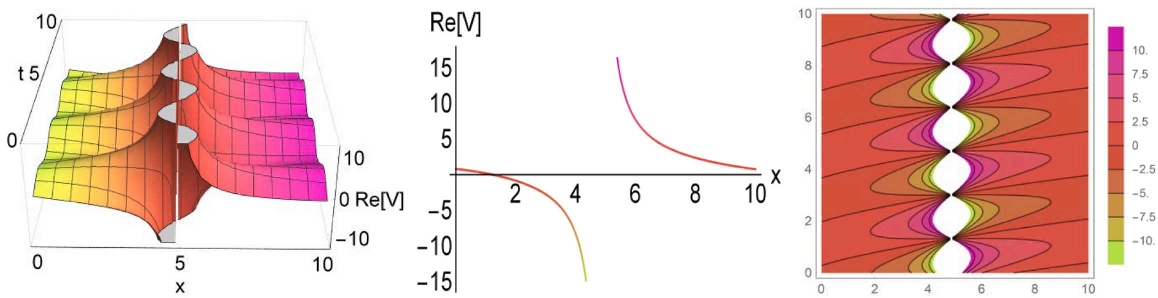

(a) 3D plot. (b) 2D plot for $t = 4$. (c) Contour plot.

Fig. 6. Graphical exhibition of the real component of solution (3.17).

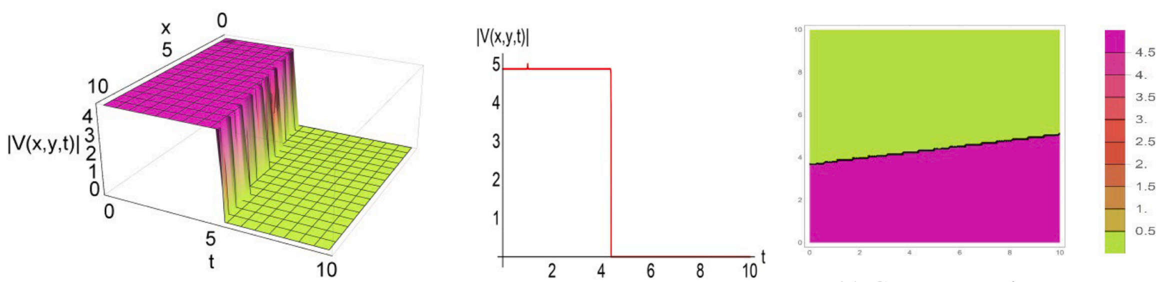

(a) 3D graph. (b) 2D graph for $x = 5$. (c) Contour graph.

Fig. 7. Graphical exhibition of the modulus of solution (3.19).

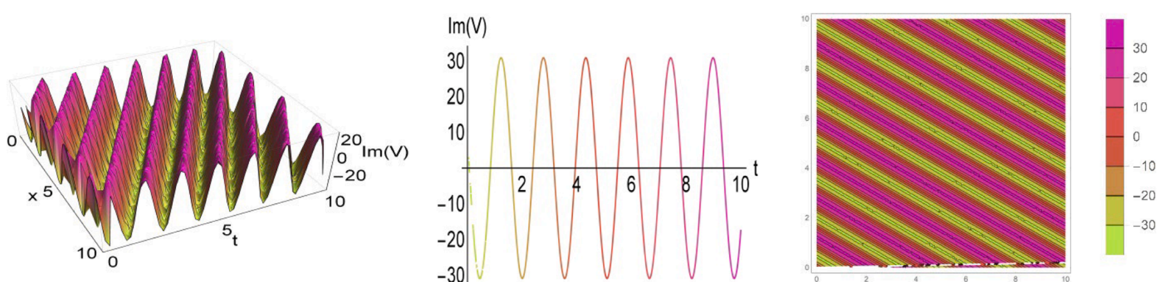

(a) 3D graph. (b) 2D graph for $x = 0$. (c) Contour graph

Fig. 8. Graphical exhibition of the imaginary component of solution (3.19).

be replicated using our approach by appropriately choosing the arbitrary constants, our method also introduces novel trigonometric and hyperbolic solutions. Unlike the separate strategies used by Cinar et al.[47], the $(G'/G,\ 1/G)$-expansion method integrates both types of solutions within a unified framework.

The aforementioned comparisons conclude the efficiency of these two methods in the extraction of solitary wave solutions from the FNLLEs, and our obtained fresh and generic results significantly increase the number of potential solutions to this equation.

5. Results and discussion

In this section, the results are plotted for various values of the physical parameters, displaying both familiar shaped solitons and recently discovered shaped solitons.

5.1. Solutions obtained from the eK method

The modulus part of (3.6) portrays a V-shaped soliton for the appropriate values of parameters $k_1 = 0.55$, $k_2 = 0.66$, $\mu = 0.8$, $\eta_1 = 5$, $\eta_2 = -4$, $\gamma_1 = 0.01$, $\gamma_2 = 0.001$, $\gamma_3 = 0.06$, $\gamma_4 = 1$, $\alpha = 0.225$, $\beta = -4$, $y = 1$ as depicted in Fig. 1. This type of soliton is also known as a dark soliton. The dark soliton can be described as a surface wave envelope that is localized and causes a temporary reduction in the amplitude of the wave. This soliton is useful in the study of the propagation of shock waves in plasma. They correspond to the minimum of both the electromagnetic energy density and the plasma density and propagate without changing their shape. In electron-ion plasmas with low propagation velocities, dark solitons have been observed, while in electron-positron plasmas, they exist as stable nonlinear coherent modes. This V-shaped soliton transforms into a flat kink soliton when η_1 changes from 5 to 1.78, as shown in Fig. 2. Additionally, the imaginary and real parts of the solution (3.6) both exhibit periodic solitons for different parameter values. Specifically, the imaginary part shows a periodic soliton in Fig. 3 for $k_1 = 1.02$, $k_2 = 0.66$, $\mu = 0.9$, , $\eta_1 = 2.7$, $\eta_2 = -4$, $\gamma_1 = 0.01$, $\gamma_2 = 0.001$, $\gamma_3 = 0$, $\gamma_4 = 1$, $\alpha = 39.4$, $\beta = -4$, and $y = 1$. Meanwhile, the Fig. 4 represents a periodic soliton in the real component of the solution for the choice of the parameters $k_1 = 2.475$, $k_2 = 1.96$, $\mu = 0.94$, $\eta_1 = 2.7$, $\eta_2 = -4$, $\gamma_1 = 0.01$, $\gamma_2 = 0.001$, $\gamma_3 = 0$, $\gamma_4 = 1$, $\alpha = 1.35$, $\beta = -4$, and $y = 1$.

Fig. 5 illustrates a singular bell-shaped soliton of the modulus of the solution (3.17) which is plotted for the values $k_1 = 0.55$, $k_2 = 0.66$, $\mu =$

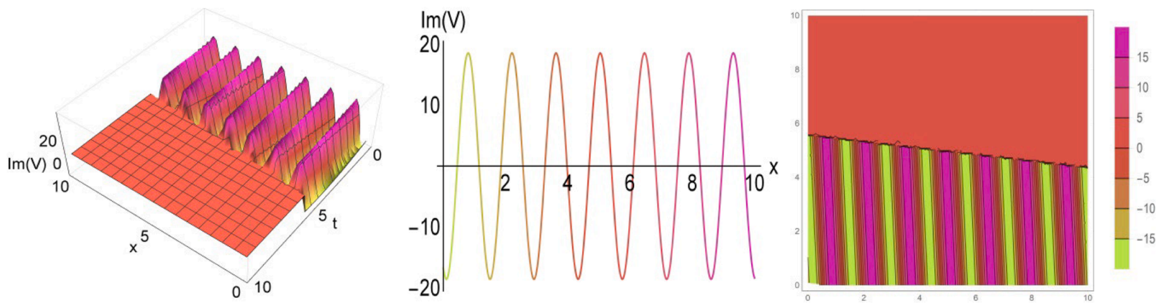

(a) 3D graph. (b) 2D graph for $t = 2$. (c) Contour graph.

Fig. 9. Graphical exhibition of the imaginary component of solution (3.20).

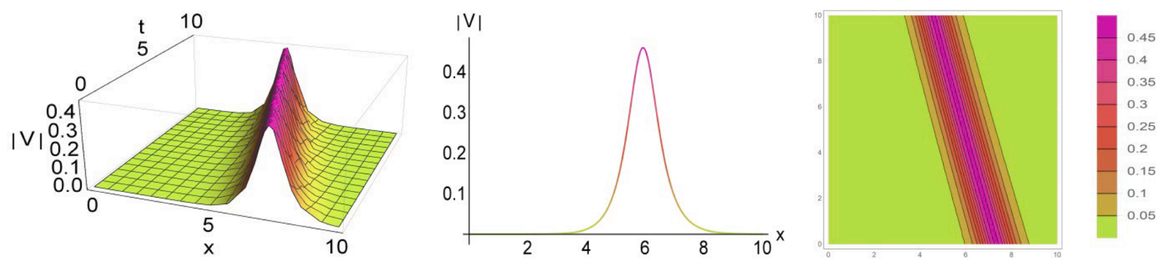

(a) 3D graph. (b) 2D graph for $t = 5$. (c) Contour graph.

Fig. 10. Graphical exhibition of the absolute component of solution (3.21).

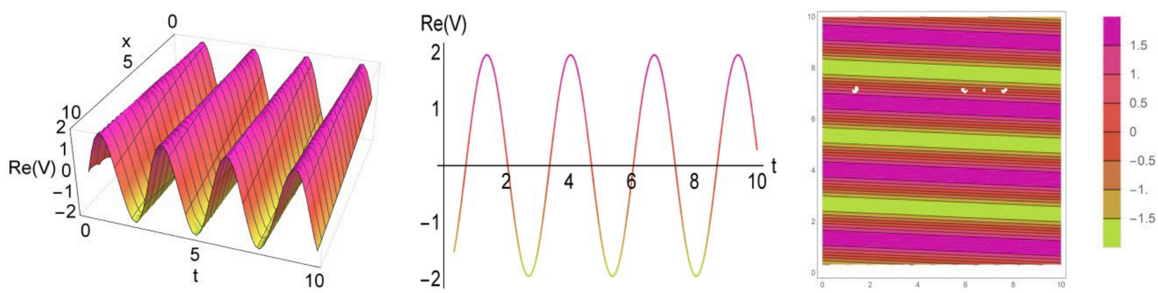

(a) 3D graph (b) 2D graph for $x = 0$. (c) Contour graph

Fig. 11. Graphical exhibition of the imaginary component of solution (3.22).

0.95, $\eta_1 = 1.7$, $\eta_2 = 4$, $\gamma_1 = 0.165$, $\gamma_2 = 0.36$, $\gamma_3 = 0.45$, $\gamma_4 = 1.29$, $R_2 = 4$, $\beta = 4$, and $y = 1$. The real component of (3.17) represents a singular periodic soliton in Fig. 6 for the values of parameters $k_1 = 0.55$, $k_2 = 0.66$, $\mu = 0.67$, $\eta_1 = 1.7$, $\eta_2 = -4$, $\gamma_1 = 4.01$, $\gamma_2 = 1.4$, $\gamma_3 = 0.1$, $\gamma_4 = 1$, $R_2 = -4$, $\beta = -2.5$, and $y = 1$.

5.2. Results attained from the $(G'/G, 1/G)$-expansion scheme

The modulus of solution (3.19) represents a kink soliton presented in Fig. 7 for the values of parameters $k_1 = 15$, $k_2 = 13.7$, $\mu = 0.99$, $\lambda = -5.25$, $\omega = 15$, $y = 0$, $\gamma_1 = 7.15$, $\gamma_2 = -3.65$, $\gamma_3 = -3.75$, $\gamma_4 = 6.2$, $g_1 = -3.08$, $g_2 = 4.36$, $\eta_1 = -13.85$, and $\delta = 0.45$, while the imaginary part of this solution depicts a periodic soliton shown in Fig. 8 for the chosen values of parameters $k_1 = -2.35$, $k_2 = -9.9$, $\mu = 0.99$, $\lambda = -4.35$, $\omega = 4.05$, $y = 0$, $\gamma_1 = -15$, $\gamma_2 = -13.5$, $\gamma_3 = -15$, $\gamma_4 = 1.85$, $g_1 = 3.46$, $g_2 = -5$, $\eta_1 = 9.65$, and $\delta = -0.35$. Kink soliton is a topological soliton that goes under a shock and sharply changes asymptotic state. From Fig. 7, it can be observed that kink soliton doesn't vanish for $t \to \infty$. Kink soliton can propagate along the chain, maintaining its shape and speed over long distances, due to the balance between the ferromagnetic interactions and the nonlinear effects that stabilize the soliton. Kink solitons are important in the study of phase transitions in ferromagnetic materials. Periodic soliton is a nonlinear wave that maintains its shape while traveling through a medium. It is a highly stable soliton that can be utilized in this context to describe lattice vibrations in condensed matter.

Fig. 9 shows the graphical exhibition of the imaginary component of the solution (3.20), which is plotted for the values $k_1 = -4.5$, $k_2 = -15$, $\mu = 0.99$, $\lambda = -2.79$, $\omega = 0.2$, $y = 0$, $\gamma_1 = -7.321$, $\gamma_2 = -4.42$, $\gamma_3 = -14.15$, $\gamma_4 = 6.1$, $g_1 = -4.4$, $g_2 = 3.91$, and $\eta_1 = -9.8$. The imaginary part of the solution (3.20) represents a flat-periodic soliton for the chosen values of parameters. From Fig. 9, we can notice that the periodic wave soliton goes under a shock at $t = 5$ and turns to a flat soliton. By studying this type of soliton, researchers can gain insight into the fundamental properties of matter and energy, and develop new technologies based on these properties. The absolute part of the outcomes in (3.21) is represented in Fig. 10 for the values $k_1 = 1.35$, $k_2 = -7.7$, $\mu = 0.79$, $\lambda = -0.99$, $\omega = 0.9$, $y = 0$, $\gamma_1 = -10.6$, $\gamma_2 = -1.15$, $\gamma_3 = -8.41$, $\gamma_4 = 9.3$, $g_1 = -2.6$, $g_2 = -3.43$, and $\eta_1 = -3.25$. The absolute value of the solution (3.21) exhibits a bell-shaped soliton, which is a potential soliton for information processing and transmitting data or energy over a distant zone without distortion. Due to its stability, it is a useful tool for understanding the dynamics of quantum systems. The solution (3.22) exhibits periodic behavior, including the absolute value, as well as the real and imaginary components. Fig. 11 includes the depiction of the imaginary component of the solution (3.22) for the values $k_1 = -0.1$, $k_2 = 1.75$, $\mu = 0.99$, $\lambda = 0.1$, $\omega = 2.35$, $y = 0$, $\gamma_1 = -15$, $\gamma_2 = -9.25$, $\gamma_3 = 11.1$, $\gamma_4 = 8.6$, $g_1 = 1.24$, $g_2 = 1.55$, $\eta_1 = 11.3$, and $\delta = 4.04$.

6. Concluding remarks

This study successfully extracted soliton solutions to the (2 + 1)-dimensional space fractional HFSC equation using the extended Kudryashov and $(G'/G, 1/G)$-expansion approaches, including the beta derivative. The derived soliton solutions involved trigonometric, rational and hyperbolic functions, each with sufficient parameters. The visualization through 3D, 2D, and contour graphs effectively illustrates various soliton types, including bell-shaped, singular bell-shaped, periodic, singular periodic, kink, and flat kink solitons. Some solutions coincide with existing ones under specific parameter values, confirming both the validity and generality of our findings. A significant number of solutions introduced in this study are original which are not found in the literature. These novel and generic solutions provide valuable insights into understanding phase transitions in ferromagnetic materials, lattice vibrations in condensed matter, and propagation of shock waves in plasma. Moreover, the extended Kudryashov and $(G'/G, 1/G)$-expansion methods have demonstrated their reliability and robustness in extracting soliton solutions for fractional order nonlinear evolution models.

Ethical approval

This article does not involve any human or animal studies. The authors affirm that they have read and adhered to the statement of ethical standards for manuscript submission to this journal. Furthermore, the manuscript has not been copyrighted, published, or submitted elsewhere.

CRediT authorship contribution statement

Sujoy Devnath: Conceptualization, Resources, Methodology, Investigation, Writing – original draft. **Mst. Munny Khatun:** Formal analysis, Validation, Visualization, Data curation, Writing – review & editing. **M. Ali Akbar:** Software, Project administration, Funding acquisition, Supervision, Writing – review & editing.

Declaration of competing interest

The authors declare that they have no known competing financial interests or personal relationships that could have appeared to influence the work reported in this article.

Data availability

No data was used for the research described in the article.

Acknowledgement

The authors would like to express their sincere gratitude to the anonymous referees for their valuable comments and suggestions, which have greatly improved the article.

References

1. Akbar MA, Abdullah FA, Khatun MM. Comprehensive geometric-shaped soliton solutions of the fractional regularized long wave equation in ocean engineering. *Alex Eng J*. 2023;72:593–604.
2. Almatrafi MB, Alharbi A. New soliton wave solutions to a nonlinear equation arising in plasma physics. *Comp Model Eng Sci*. 2023;137(1):827–841.
3. Kumar S, Mohan B. A novel analysis of Cole-Hopf transformations in different dimensions, solitons, and rogue waves for a (2+1)-dimensional shallow water wave equation of ion-acoustic waves in plasmas. *Phys fluids*. 2023;35(12), 127128.
4. Devnath S, Akbar MA, Gómez-Aguilar JF. Diverse optical soliton solutions of two space-time fractional nonlinear evolution equations by the extended Kudryashov method. *Phys Scr*. 2023;98(11), 115235.
5. Ma CY, Shiri B, Wu GC, Baleanu D. New fractional signal smoothing equations with short memory and variable order. *Optik (Stuttg)*. 2020;218, 164507.
6. Kumar S, Niwas M. New optical soliton solutions of Biswas-Arshed equation using the generalized exponential rational function approach and Kudryashov's simplest equation approach. *Pramana-J Phys*. 2022;96(4):204.
7. Kukkar A, Kumar S, Malik S, et al. Optical solitons for the concatenation model with Kudryashov's approaches. *Ukrainian J Phys Optic*. 2023;24(2):155–160.
8. Khan AQ, Almatrafi MB. Two-dimensional discrete-time laser model with chaos and bifurcations. *AIMS Math*. 2023;8:6804–6828.
9. Nestor S, Abbagari S, Houwe A, Inc M, Betchewe G, Doka SY. Diverse chirped optical solitons and new complex traveling waves in nonlinear optical fibers. *Commun Theor Phys*. 2020;72, 065501.
10. Su X, Chen W, Xu W. Characterizing the rheological behaviors of non-Newtonian fluid via a viscoelastic component: fractal dashpot. *Adv Mech Eng*. 2017;9(10):1–12.
11. Ryehan S. Numerically unveiling hidden chaotic dynamics in nonlinear differential equations with Riemann-Liouville, Caputo-Fabrizio, and Atangana-Baleanu Fractional derivatives. arXiv preprint arXiv:2307.03251 2023.
12. Suzuki JL, Gulian M, Zayernouri M, D'Elia M. Fractional modeling in action: a survey of nonlocal models for subsurface transport, turbulent flows, and anomalous materials. *J Peridyn Nonlocal Model*. 2023;5(3):392–459.
13. Han B, Yin D, Gao Y. The application of a novel variable-order fractional calculus on rheological model for viscoelastic materials. *Mech Adv Mater Struct*. 2023;11:1–3.
14. Wang Q, Ma J, Yu S, Tan L. Noise detection and image denoising based on fractional calculus. *Chaos Solitons Fractals*. 2020;131, 109463.
15. De Oliveira ECT, Machado JA. A review of definitions for fractional derivatives and integral. *Math Probl Eng*. 2014;2014:1–6.
16. Almatrafi MB. Construction of closed form soliton solutions to the space-time fractional symmetric regularized long wave equation using two reliable methods. *Fractals*. 2023;31(10), 2340160.
17. Khalil R, Al Horani M, Yousef A, Sababheh M. A new definition of fractional derivative. *J Comput Appl Math*. 2014;264:65–70.
18. Berkal M, Almatrafi MB. Bifurcation and stability of two-dimensional activator–inhibitor model with fractional order derivative. *Fractal Fract*. 2023;7(5): 344.
19. Atangana A, Baleanu D, Alsaedi A. Analysis of time-fractional Hunter-Saxton equation: a model of neumatic liquid crystal. *Open Phys*. 2016;14(1):145–149.
20. Abdelhakim AA, Machado JA. A critical analysis of the conformable derivative. *Nonlinear Dyn*. 2019;95:3063–3073.
21. Devnath S, Khan K, Akbar MA. Numerous analytical wave solutions to the time-fractional unstable nonlinear Schrödinger equation with beta derivative. *Partial Differ Equ Appl Math*. 2023;8, 100537.
22. Bakıcıerler G, Alfaqeih S, Mısırlı E. Analytic solutions of a (2+1)-dimensional nonlinear Heisenberg ferromagnetic spin chain equation. *Phys A: Stat Mech*. 2021; 582, 126255.
23. Nakane R, Tanaka G, Hirose A. Reservoir computing with spin waves excited in a garnet film. *IEEE*. 2018;6:4462–4469.
24. Latha MM, Vasanthi CC. An integrable model of (2+1)-dimensional Heisenberg ferromagnetic spin chain and soliton excitations. *Phys Scr*. 2014;89(6), 065204.
25. Houwe A, Abbagari S, Doka SY, Inc M, Bouetou TB. Clout of fractional time order and magnetic coupling coefficients on the soliton and modulation instability gain in the Heisenberg ferromagnetic spin chain. *Chaos Solitons Fractals*. 2021;151, 111254.
26. Uddin MF, Hafez MG, Hammouch Z, Baleanu D. Periodic and rogue waves for Heisenberg models of ferromagnetic spin chains with fractional beta derivative evolution and obliqueness. *Waves Random Complex Media*. 2021;31(6):2135–2149.
27. Seadawy AR, Nasreen N, Lu D, Arshad M. Arising wave propagation in nonlinear media for the (2+1)-dimensional Heisenberg ferromagnetic spin chain dynamical model. *Phys A: Stat Mech*. 2020;538, 122846.
28. Hashemi MS. Some new exact solutions of (2+1)-dimensional nonlinear Heisenberg ferromagnetic spin chain with the conformable time fractional derivative. *Opt Quantum Electron*. 2018;50(2):79.
29. Hosseini K, Kaur L, Mirzazadeh M, Baskonus HM. 1-Soliton solutions of the (2+1)-dimensional Heisenberg ferromagnetic spin chain model with the beta time derivative. *Opt Quantum Electron*. 2021;53:1–10.
30. İnç M, Aliyu AI, Yusuf A, Baleanu D. Optical solitons and modulation instability analysis of an integrable model of (2+1)-dimensional Heisenberg ferromagnetic spin chain equation. *Superlattices Microstruct*. 2017;112:628–638.
31. Bashar MH, Islam SR, Kumar D. Construction of traveling wave solutions of the (2+1)-dimensional Heisenberg ferromagnetic spin chain equation. *Partial Differ Equ Appl Math*. 2021;4, 100040.
32. Tuluce DS, Bayrakci U. Soliton solutions for space-time fractional Heisenberg ferromagnetic spin chain equation by generalized Kudryashov method and modified exp (-Ω (η))-expansion function method. *Rev Mex de Fis*. 2021;67(3):393–402.
33. Zhao XH, Tian B, Liu DY, Wu XY, Chai J, Guo YJ. Dark solitons interaction for a (2+1)-dimensional nonlinear Schrödinger equation in the Heisenberg ferromagnetic spin chain. *Superlattices Microstruct*. 2016;100:587–595.
34. Guan B, Chen S, Liu Y, Wang X, Zhao J. Wave patterns of (2+1)-dimensional nonlinear Heisenberg ferromagnetic spin chains in the semiclassical limit. *Results Phys*. 2020;16, 102834.
35. Alharbi AR, Almatrafi MB. Exact solitary wave and numerical solutions for geophysical KdV equation. *J King Saud Univ Sci*. 2022;34(6), 102087.

36. Islam T, Akbar MA, Azad AK. Traveling wave solutions to some nonlinear fractional partial differential equations through the rational (G′/G)-expansion method. *J Ocean Eng. Sci*. 2018;3(1):76–81.
37. Devnath S, Khan S, Akbar MA. Exploring solitary wave solutions to the simplified modified camassa-holm equation through a couple sophisticated analytical approaches. *Results Phys*. 2024;59, 107580.
38. Khatun MM, Akbar MA. Analytical soliton solutions of the beta time-fractional simplified modified Camassa-Holm equation in shallow water wave propagation. *J Umm Al-Qura Univ Appl Sci*. 2024;10:120–128.
39. Niwas M, Dhiman SK, Kumar S. Dynamical forms of various optical soliton solutions and other solitons for the new Schrödinger equation in optical fibers using two distinct efficient approaches. *Mod Phys Lett B*. 2024;38(13), 2450087.
40. Kumar S, Mann N. Abundant closed-form solutions of the (3+1)-dimensional Vakhnenko-Parkes equation describing the dynamics of various solitary waves in ocean engineering. *J Ocean Eng Sci*. 2022 (in press).
41. Ahmed R, Almatrafi MB. Complex dynamics of a predator-prey system with Gompertz growth and herd behavior. *Int J Anal Appl*. 2023;21:100.
42. Alharbi AR, Almatrafi MB. New exact and numerical solutions with their stability for Ito integro-differential equation via Riccati-Bernoulli sub-ODE method. *J Taibah Univ Sci*. 2020;14(1):1447–1456.
43. Kumar S, Mohan B. A generalized nonlinear fifth-order KdV-type equation with multiple soliton solutions: painlevé analysis and Hirota Bilinear technique. *Phys Scr*. 2022;97(12), 125214.
44. Kumar S, Mohan B, Kumar R. Lump, soliton, and interaction solutions to a generalized two-mode higher-order nonlinear evolution equation in plasma physics. *Nonlinear Dyn*. 2022;110(1):693–704.
45. Mohan B, Kumar S, Kumar R. Higher-order rogue waves and dispersive solitons of a novel P-type (3+1)-dimensional evolution equation in soliton theory and nonlinear waves. *Nonlinear Dyn*. 2023;111(21):20275–20288.
46. Almatrafi MB. Solitary wave solutions to a fractional model using the improved modified extended tanh-function method. *Fractal Fract*. 2023;7(3):252.
47. Cinar M, Onder I, Secer A, et al. Soliton Solutions of (2+1) Dimensional Heisenberg ferromagnetic spin equation by the extended rational sine-cosine sine-cosine and sinh-cosh sinh-cosh method. *Int J Appl Comput Math*. 2021;7:1–7.